THE ROYAL SOCIETY

One-dimensional numerical simulations of idealized detonations

By G. J. Sharpe and S. A. E. G. Falle

Department of Applied Mathematical Studies, University of Leeds, Leeds LS2 9JT, UK

Received 15 January 1998; accepted 23 June 1998

In this paper we use a second-order Godunov scheme to perform one-dimensional time-dependent numerical simulations of an idealized Chapman–Jouguet detonation having an Arrhenius form of reaction rate. The evolution of the longitudinal instability is explored for varying activation temperatures and compared to predictions of a linear stability analysis of the steady detonation. We show that, for large enough activation temperature, the detonation propagates in a series of failures followed by reignition, which can lead to the formation of many large pockets of partly burnt fuel. These results are in disagreement with the previous results of He & Lee, although we find that we can reproduce their results when too coarse a numerical grid is used.

Keywords: Chapman–Jouguet; stability of detonations; Godunov

1. Introduction

A detonation is a rapid regime of burning in which a strong shock ignites the fuel and the burning proceeds to equilibrium behind the shock, while the energy released continues to drive the shock. This process can be modelled mathematically by the reactive Euler equations, which express the conservation laws of mass, momentum, energy and rate of fuel (reactant) consumption. These equations have solutions, the so-called Zeldovich–Neumann–Döring (ZND) waves, in which the detonation is steady, one-dimensional and planar. However, experiments (see, for example, Fickett & Davis 1979) reveal that detonation fronts usually have a complicated three-dimensional time-dependent structure with interior transverse waves. 'Galloping' detonations, in which the front oscillates longitudinally, occur when blunt bodies move through a reactive gas at near-Chapman–Jouguet (CJ) velocities. In round tubes, 'spinning' detonations are observed in which the transverse waves rotate about the tube axis. Perhaps of most interest are the cellular detonations that appear in rectangular tubes. If the tube width is not very much larger than the length-scale of the reaction, the detonation can create remarkably regular diamond-shaped patterns in soot deposited on the walls of the tubes. In these cases it is clear that the ZND waves are unstable to small perturbations in the flow.

Although this time-dependent three-dimensional phenomenon is not amenable to analysis, it is possible to carry out a linear stability analysis of the ZND solutions. The linear stability analysis of steady planar detonations was pioneered by Erpenbeck (1962). Recently, Sharpe (1997) developed a new normal mode approach to the linear stability problem and applied it to an idealized detonation with a single reaction. This method was found to be superior to that of previous workers in the sense that

not only was the CJ case, for the first time, well posed, but it also allowed the linear spectrum to be found for much higher values of the activation temperature.

Fickett & Wood (1966) have computed time-dependent one-dimensional idealized overdriven detonations using the method of characteristics. They investigated the behaviour of detonations near the neutral stability curve for one-dimensional perturbations given by Erpenbeck (1964) and found that their results agreed with his stability criterion. Although the post-shock pressure did initially oscillate, these oscillations were quickly damped out and the wave reverted to the ZND solution on the stable side of the stability curve, but they did not do so on the unstable side. Furthermore, they found that, for unstable detonations near the stability boundary, the frequency of the oscillations was quite close to that predicted by the linear stability analysis. This has led several authors to use results of the linear stability analysis for longitudinal perturbations to test their numerical schemes (see, for example, Bourlioux *et al*. 1991).

He & Lee's (1995) one-dimensional computations explored the behaviour of detonations further from the stability boundary than previous authors. They found that as the degree of overdrive is decreased, or the activation energy is increased for the CJ case, the nature of the pulsations change as one moves away from the stability boundary. Near the boundary the pulsations are regular and harmonic, but they become nonlinear and then chaotic further from the boundary until a point is reached after which pulsating one-dimensional detonations cannot propagate. In these very unstable cases the leading shock becomes very weak and decouples from the reaction front for long periods of time. They suggested that this limit occurs when the linear fundamental mode becomes non-oscillatory.

In this paper we present one-dimensional, time-dependent, high-resolution numerical simulations of CJ detonations using a second-order Godunov scheme. At large activation temperatures, our solutions differ from those of He & Lee (1995) in that they show the formation of large pockets of partly burnt fuel, a phenomenon which has previously only been seen in two-dimensional simulations. The fact that we are able to recover their results by using a coarser grid suggests that this discrepancy is simply due to inadequate numerical resolution in their calculations.

The plan of the paper is as follows: § 2 gives the governing equations, and defines the non-dimensional variables; § 3 summarizes the results of a linear stability analysis; the numerical results are presented in § 4; § 5 contains the conclusions and some suggestions for future work.

2. Governing equations

In one dimension, the governing equations for our idealized detonation are

$$\left.\begin{aligned} \frac{\partial \rho}{\partial t}+\frac{\partial(\rho u)}{\partial x}=0, \qquad & \frac{\partial(\rho u)}{\partial t}+\frac{\partial(p+\rho u^2)}{\partial x}=0, \\ \frac{\partial E}{\partial t}+\frac{\partial(Eu+pu)}{\partial x}=0, \qquad & \frac{\partial(\rho\lambda)}{\partial t}+\frac{\partial(\rho u\lambda)}{\partial x}=W, \end{aligned}\right\} \tag{2.1}$$

where u is the fluid velocity in the laboratory frame, ρ is the density, p is the pressure, E is the total energy per unit volume, λ is the reaction progress variable (with $\lambda = 1$ for unburnt and $\lambda = 0$ for burnt fuel) and $W \equiv W(\rho, p, \lambda)$ is the reaction rate. We

assume an Arrhenius form of the reaction rate and a perfect gas, so that

$$E = \frac{p}{\gamma - 1} + \tfrac{1}{2}\rho u^2 - \rho Q(1 - \lambda)$$

and

$$W = -K\rho\lambda \mathrm{e}^{(-T_\mathrm{A}/T)}, \qquad T = \frac{\mu p}{R\rho},$$

where Q is the (constant) heat of reaction, γ is the (constant) ratio of specific heats, T is the temperature, T_A is the activation temperature, K is a constant rate coefficient, R is the universal gas constant and μ is the mean molecular weight.

Henceforth we use a bar ($\bar{}$) to denote dimensional quantities, a zero (0) subscript to denote quantities in the steady wave and a minus ($-$) superscript to denote quantities ahead of the shock. We non-dimensionalize by putting

$$\rho = \frac{\bar\rho}{\bar\rho_0^-}, \quad \boldsymbol{v} = \frac{\bar{\boldsymbol{v}}}{\bar D}, \quad p = \frac{\bar p}{\bar\rho_0^-\bar D^2}, \quad T = \frac{p}{\rho} = \frac{\bar R\bar T}{\bar\mu\bar D^2} \quad \text{with} \quad \tau = \frac{\bar R\bar T_\mathrm{A}}{\bar\mu\bar D^2}, \quad t = \frac{\bar K\bar t}{\alpha},$$
$$\boldsymbol{r} = \frac{\bar K\bar{\boldsymbol{r}}}{\alpha\bar D}, \quad Q = \frac{\bar Q}{\bar D^2},$$

where $\bar D$ is the CJ speed of the steady detonation wave, τ is the non-dimensional activation temperature and α is a scale factor chosen so that the characteristic length-scale is the half-reaction length of the steady wave, i.e. the point at which $\lambda = \frac{1}{2}$.

In terms of these non-dimensional variables, equations (2.1) are unchanged in form except that the reaction rate is now given by

$$W = -\alpha\rho\lambda \exp(-\tau\rho/p).$$

We also define

$$P = \frac{\bar p_0^-}{\bar\rho_0^-\bar D^2},$$

i.e. the non-dimensional pressure in the ambient material. Note that

$$\bar Q = \frac{(\bar\rho_0^-\bar D^2 - \gamma\bar p_0^-)^2}{2(\bar\rho_0^-)^2\bar D^2(\gamma^2 - 1)},$$

so that

$$Q = \frac{(1 - \gamma P)^2}{2(\gamma^2 - 1)}.$$

Previous workers have scaled the activation temperature and heat of reaction by defining

$$E = \frac{\bar T_\mathrm{A}}{\bar T_0^-} \quad \text{and} \quad Q^* = \frac{\bar Q\bar\mu}{\bar R\bar T_0^-},$$

where $\bar T_0^-$ is the dimensional temperature in the ambient material. Note that

$$\bar T_0^- = \frac{\bar\mu\bar p_0^-}{\bar R\bar\rho_0^-} = \frac{\bar\mu}{\bar R}\bar D^2 P,$$

Table 1. *Linear eigenvalues for various values of the activation temperature* ($P = 0.0216$, $\gamma = 1.2$.)

τ	eigenvalues		
0.545	$0.0000 + 0.0779$i		
0.550	$0.0018 + 0.0775$i		
0.600	$0.0183 + 0.0723$i		
0.650	$0.0336 + 0.0636$i		
0.670	$0.0394 + 0.0591$i	$0.0000 + 0.643$i	
0.700	$0.0478 + 0.0507$i	$0.0281 + 0.643$i	
0.750	$0.0609 + 0.0295$i	$0.0704 + 0.641$i	
0.773	$0.0668 + 0.0000$i	$0.0882 + 0.640$i	$0.0000 + 1.160$i
0.800	$0.0413, 0.105$	$0.108 + 0.638$i	$0.0324 + 1.161$i

so that

$$E = \frac{\bar{R}\bar{T}_{\mathrm{A}}}{\bar{\mu}\bar{D}^2 P} = \frac{\tau}{P}$$

and

$$Q^* = \frac{\bar{Q}}{\bar{D}^2 P} = \frac{Q}{P} = \frac{(1-\gamma P)^2}{2(\gamma^2 - 1)P}.$$

In this paper we set $\gamma = 1.2$ and $P = 0.0216$ (corresponding to $Q^* = 50$).

3. Results from the linear stability analysis

In order to compare the numerical results with the predictions of the linear stability analysis, the method of Sharpe (1997) was used to find the one-dimensional linear spectrum for various activation temperatures.

Table 1 gives the eigenvalues for the range of activation temperatures used in the numerical simulations. Below $\tau = 0.545$ there are no (unstable) modes so that the steady detonation is stable. At $\tau = 0.545$ the fundamental mode becomes unstable. The growth rate of this mode increases with activation temperature and its frequency decreases. The second and third modes become unstable at $\tau = 0.670$ and $\tau = 0.773$, respectively. The fundamental mode splits into two real (non-oscillatory) eigenvalues, also at $\tau = 0.773$. One of these eigenvalues decreases asymptotically to zero, while the other increases rapidly with increasing activation temperature. Although the growth rates of the higher modes initially increase with activation temperature, Sharpe (1997) found that at sufficiently high activation temperatures their growth rates begin to decrease and then converge to a limit. The spectrum is then dominated by the very large real eigenvalue associated with the fundamental mode.

4. Numerical simulations

In this paper we use a second-order (in space and time) Godunov (1959) scheme with uniform mesh spacing to perform the numerical simulations. The scheme is described in Falle (1991).

In our simulations the detonation runs from left to right in the positive x-direction. Since the fluid ahead of the detonation is in its quiescent state, this means that the right-hand boundary condition is irrelevant provided the shock remains within the domain. The boundary condition on the left is more difficult. Both He & Lee (1995) and Bourlioux *et al*. (1991) impose the steady-state solution. This is a somewhat dubious procedure for unstable detonations and only remains valid as long as no perturbations reach the boundary. It might be better to impose a zero-gradient condition, but this would also not be correct if the instability produces steep gradients near the boundary. We therefore place the left boundary at $x = -100$, which is far enough behind the initial position of the front to ensure that no perturbations reach it during the calculation.

The initial data are given by the steady solution, with the shock initially at $x = 0$ and the detonation lying to the left. The numerical scheme spreads the initially discontinuous shock over a few grid cells and this introduces a perturbation that is sufficient to trigger the instability.

The reactive Euler equations require much finer grids than those without reaction because of the stiff nature of the chemical source terms. Too coarse a mesh can give an incorrect detonation wave speed and can predict that the detonation is stable when in reality it may be unstable. For their one-dimensional simulations both He & Lee (1995) and Bourlioux *et al*. (1991) found that about 10 grid points per half-reaction length were required for good results near the stability boundary. Note that the size of the initial perturbation also depends on the mesh spacing. For each case the mesh is repeatedly refined until the qualitative nature of the evolution of the perturbation does not change and any sharp features that appear in the flow (shocks, reaction fronts) are well resolved. As the activation temperature is increased, finer and finer meshes are required.

(*a*) *Results*

The linear stability analysis predicts that detonations with activation temperatures less than $\tau = 0.545$ are stable. Figure 1 shows the post-shock pressure versus time for activation temperatures near the stability boundary. Ten points per half-reaction length were used in these simulations. For $\tau = 0.5$ (figure 1*a*) the initial perturbation is quickly damped out and the detonation returns to the steady state. Figure 1*b* shows that for $\tau = 0.54$ the detonation is still stable but it takes much longer for the initial perturbation to decay. Figure 1*c* shows the post-shock pressure history for $\tau = 0.55$. For this value of the activation temperature there is a single unstable linear eigenvalue, $\sigma = 0.0018 + 0.0775\mathrm{i}$. The amplitude of the post-shock pressure oscillations initially grows and then saturates. The period of the oscillations is about 80, which is in good agreement with the linear stability prediction of $2\pi/0.0775 = 81.07$.

Figure 2 shows the post-shock pressure histories for $\tau = 0.6$ and $\tau = 0.65$. Twenty points per half-reaction length were used for these cases. The post-shock pressure for $\tau = 0.6$ no longer oscillates regularly. The peak-to-peak period varies from 75 to 100. The linear spectrum has a single eigenvalue $\sigma = 0.0183 + 0.0723\mathrm{i}$, which corresponds to a period of 86.90. Clearly, nonlinear effects have already become important.

As can be seen from figure 2*b*, for $\tau = 0.65$ the behaviour changes yet again. After an initial large oscillation the post-shock pressure drops to a low level and the reaction

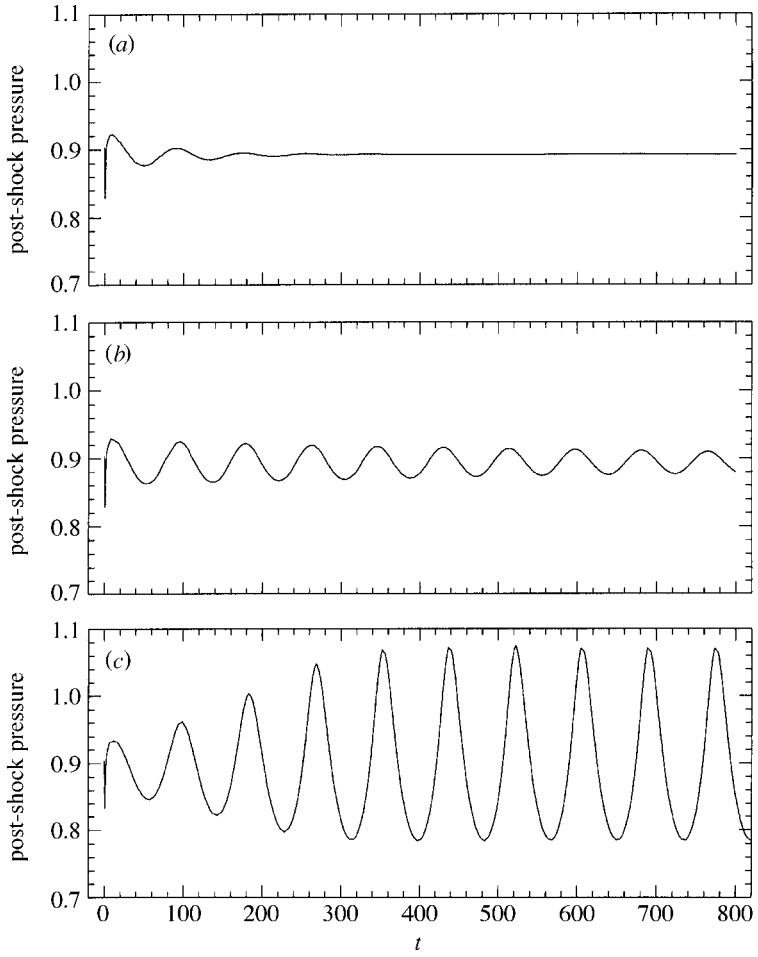

Figure 1. Post-shock pressure history for the activation temperatures (*a*) $\tau = 0.5$, (*b*) $\tau = 0.54$ and (*c*) $\tau = 0.55$.

zone starts to decouple from the shock. After an induction time a reignition takes place with the reaction zone rapidly accelerating towards the shock. This 'explosion within the explosion' quickly catches up with the leading shock and produces a very high post-shock pressure. Such a high shock pressure cannot be maintained once the gas has burned and it rapidly drops to about the steady value, producing a backward-facing shock. Figure 3*a* shows profiles of the pressure during the reignition at intervals of 320 time-steps. A similar event occurs at around $t = 800$: the detonation begins to die, but later a rapid explosion occurs. Figure 3*b* shows the pressure profile between $t = 713.6$ and $t = 813.5$. However, in this case a small kink appears in the profile of λ, as can be seen in figure 4, which shows profiles of λ from $t = 796.1$ to $t = 802.0$ at intervals of 64 time-steps. The kink is caused by particles of gas being shocked at different temperatures and thus taking different times to burn. Such pockets of partly burnt gas have not been reported by previous workers. Note that at small early times, high-frequency oscillations, which are soon damped out, can be seen in

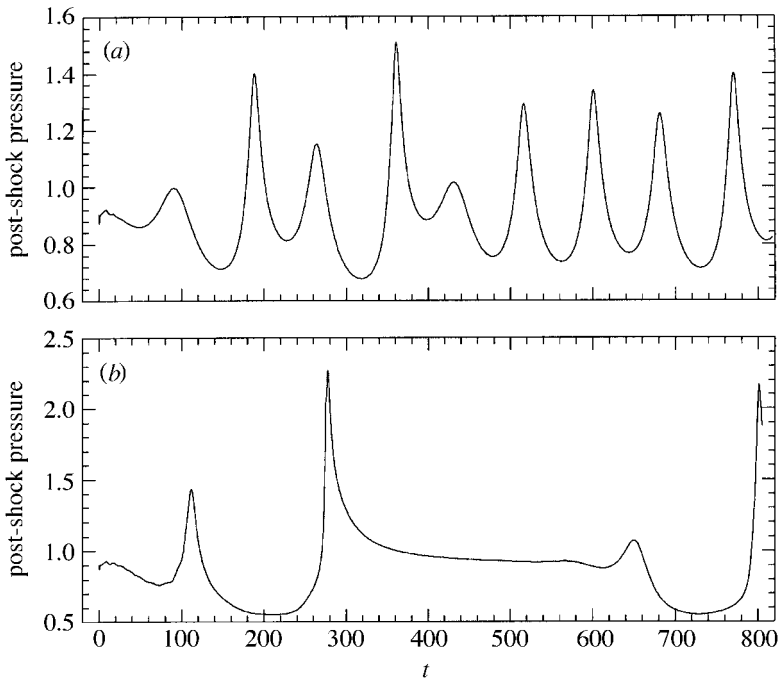

Figure 2. Post-shock pressure history for the activation temperatures (*a*) $\tau = 0.6$ and (*b*) $\tau = 0.65$.

the post-shock pressure history. For this case the linear spectrum still has a single eigenvalue: $\sigma = 0.0336 + 0.0636\mathrm{i}$.

Figure 5*a* shows the post-shock pressure history for $\tau = 0.7$. In this case the linear spectrum has two eigenvalues: $\sigma = 0.0478 + 0.0507\mathrm{i}$ and $\sigma = 0.0281 + 0.643\mathrm{i}$. The high-frequency oscillations at early times, which were damped for $\tau = 0.65$, grow for $\tau = 0.7$ with a period of about 10. These clearly correspond to the second mode, which has a predicted period of 9.77, and are superimposed on the decay of the detonation. Later the detonation begins to reignite in a series of explosions within the explosion. Again pockets of partly burnt gas are formed by these events. Figure 6 shows profiles of λ at various times. The pockets are now quite large and are sandwiched between regions of completely burnt gas. The pockets fall further and further behind the front and produce forward- and backward-facing shocks as they burn out. Around $t = 310$ a large explosion causes the post-shock pressure and temperature to increase sharply and reach large values, ending the cycle of failure followed by reignition. The post-shock pressure then drops off rapidly and the remaining pockets of partly burnt gas quickly burn out. A forward-facing shock catches up with the front, causing a slight increase in speed followed by a slow decay until at $t = 485$ a stronger forward-facing shock overtakes the front, which causes the detonation to go into an oscillating regime. The period of these oscillations is much shorter than that associated with the first linear eigenvalue and much longer than that of the second. It it unclear how long the oscillations persist. However, the final forward-facing shock will eventually overtake the front, which may cause the behaviour of the detonation to change again.

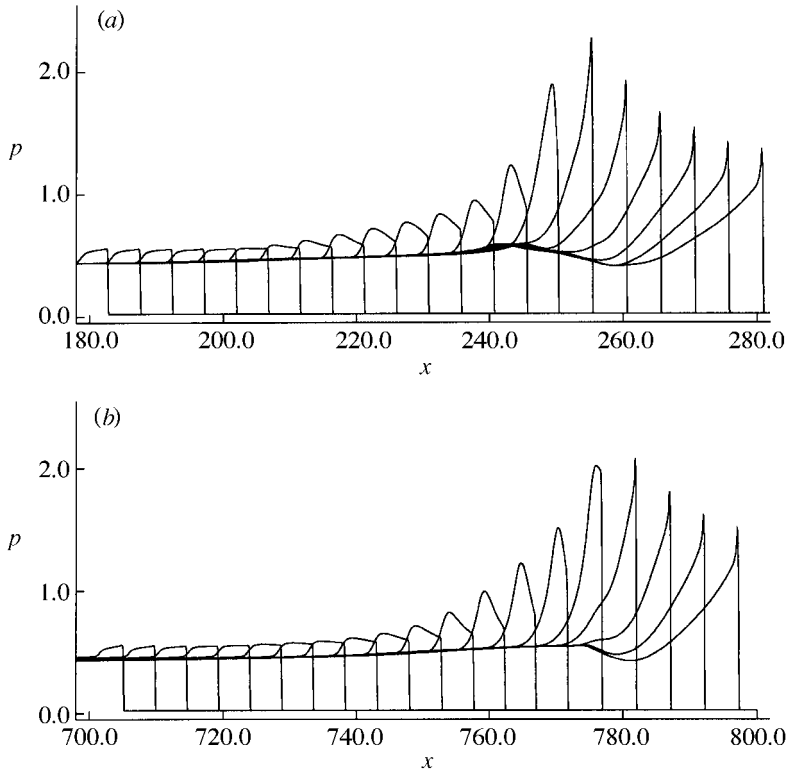

Figure 3. Pressure profiles for $\tau = 0.65$ from (a) $t = 192.3$ to $t = 296.2$ and (b) $t = 713.6$ to $t = 813.5$.

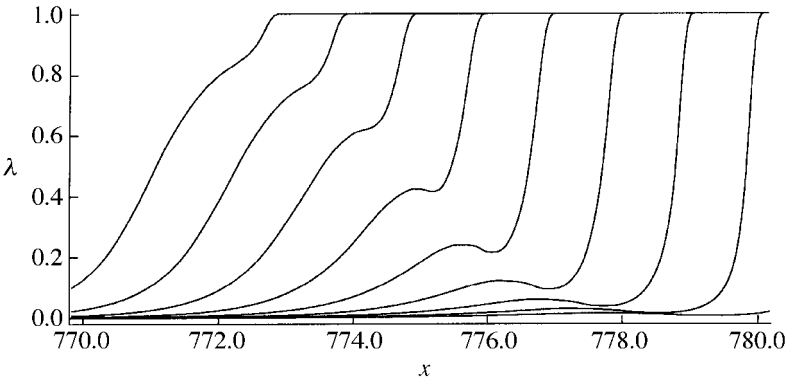

Figure 4. Profiles of λ for $\tau = 0.65$ from $t = 796.1$ to $t = 802.0$.

This behaviour for $\tau = 0.7$ is quite different from that described by He & Lee (1995). They studied both the effects of increasing the activation temperature and decreasing the degree of overdrive. They found there was a transition from irregular and chaotic oscillating detonations to a regime in which the detonation quickly died with the shock and reaction zone becoming decoupled. The flow remained in this state for some time until a rapid reignition raised the pressure to high values again. The time at which the reignition occurred increased dramatically with increasing

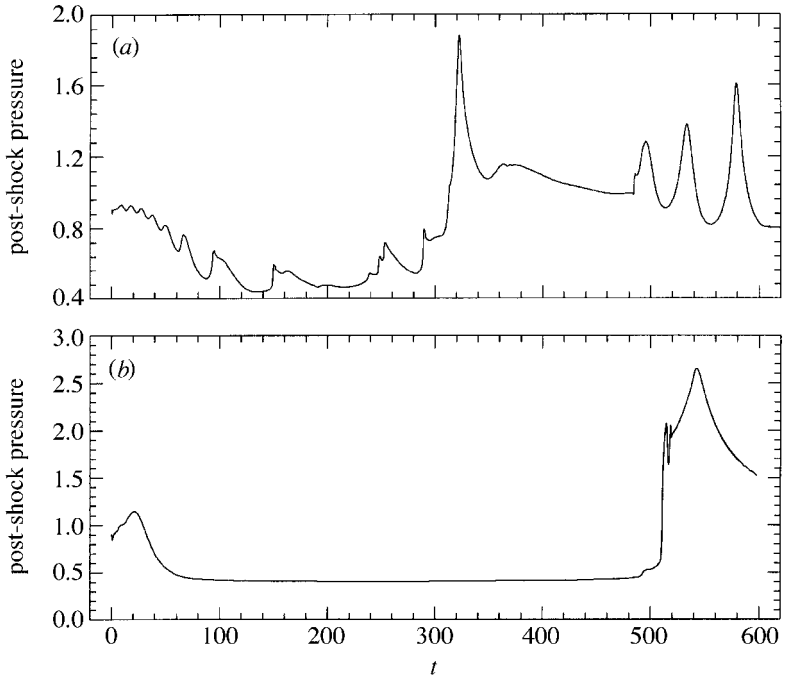

Figure 5. Post-shock pressure history for $\tau = 0.7$ with (a) 30 grid points per half-reaction length and (b) 10 grid points per half-reaction length.

activation temperature or decreasing overdrive. They suggested that at some value the detonation will never be reignited and that this occurs near the point where the fundamental linear eigenvalue becomes non-oscillatory. Figure 5*b* shows that we get very similar behaviour for $\tau = 0.7$ when there are only 10 grid points per half-reaction length. This is not enough to allow the pockets of partly burnt gas to form since they do so on scales less than a cell size. Also, the high-frequency oscillations seen with more refined meshes are suppressed when a coarse grid is used.

However, like He & Lee (1995), we find that the intervals between the deaths and the subsequent reignitions do indeed increase with increasing activation temperature. Figure 7 shows the post-shock pressure history for $\tau = 0.8$ using 50 grid points per half-reaction length. The post-shock pressure now remains low for quite long periods of time and small reignitions occur infrequently. For such high activation temperatures an explosion that raises the post-shock pressure to high values will occur at very late times, if at all: there may not be a series of explosions strong enough to do so. If so the detonation will propagate indefinitely as a series of deaths interspersed with small explosions. This transition may occur in the neighbourhood of the value of the activation temperature where the fundamental linear mode becomes non-oscillatory ($\tau = 0.773$ in this case).

The behaviour of the instability at high activation temperatures may correspond to the 'slow gallop' instability observed in square tubes, where the detonation decays to a flame lagging behind the shock with the detonation being reignited again by a deflagration–detonation transition (Fickett & Davis 1979).

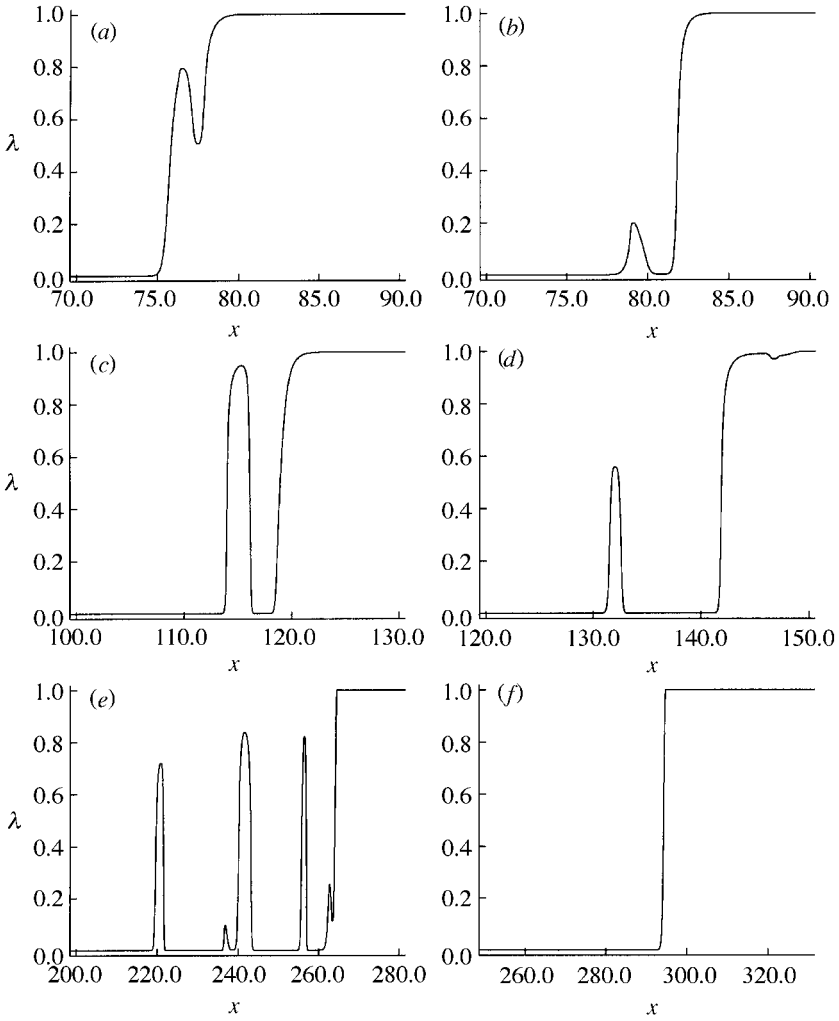

Figure 6. Profiles of λ for $\tau = 0.7$ at times (*a*) $t = 85.4$, (*b*) $t = 90.8$, (*c*) $t = 142.6$, (*d*) $t = 177.2$, (*e*) $t = 320.4$ and (*f*) $t = 345.0$.

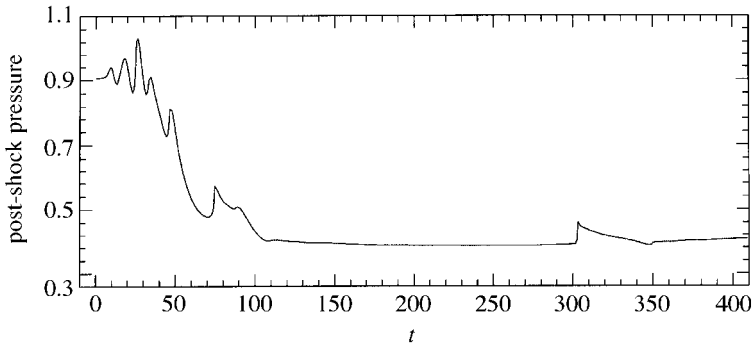

Figure 7. Post-shock pressure history for $\tau = 0.8$.

5. Conclusions

For low activation temperatures our results are consistent both with previous numerical calculations and the neutral stability boundary given by the linear stability analysis. For unstable detonations very near the stability boundary, the linear stability analysis also provides very good predictions of the final frequency of the oscillations. However, as the activation temperature is increased, the oscillations become increasingly irregular and more strongly influenced by nonlinear effects. At an even higher activation temperature the detonation propagates as a series of explosions. The times between these explosions increase markedly with increasing activation temperature and the fluctuation in the reaction rate is sufficient to allow the formation of pockets of partly burnt fuel. This has not been reported before in such one-dimensional simulations; indeed, He & Lee (1995) found that the detonation dies and remains at low pressures for very long periods of time. We have only been able to reproduce their results by using a coarser grid. This suggests that the series of explosions was suppressed in their calculations, even though they did use higher numerical resolution for the more unstable detonation. Finally, it seems that even in the nonlinear regime the evolution is dominated by the fundamental mode of instability and that the higher frequency modes are only significant at early times.

Not only is it gratifying that the calculations agree so well with the linear stability analysis, but we have also discovered some interesting behaviour for large activation energies. Although one might expect real detonations to be dominated by multidimensional instabilities, the decay and reignition in our numerical results looks very similar to the 'slow gallop' instability that is sometimes observed in square tubes (Fickett & Davis 1979). However, this phenomenon is very rare and detonations usually exhibit three-dimensional instabilities, which make them behave in a completely different way. For example, the cellular structure that can form in multidimensions may constantly reignite the detonation and thus prevent it from dying for long periods. However, the one-dimensional simulations show that very high resolution is required, which in more than one dimension can only be attained by adaptive gridding techniques such as those developed by Falle & Giddings (1993), Bourlioux & Majda (1995) and Quirk (1994). Also, as pointed out by He & Lee (1995), the dependence of such two-dimensional simulations on initial and boundary conditions needs to be explored further.

This work was carried out while G.J.S. was in receipt of an EPSRC studentship.

References

Bourlioux, A. & Majda, A. J. 1995 Theoretical and numerical structure of unstable detonations. *Phil. Trans. R. Soc. Lond.* A **350**, 29–68.

Bourlioux, A., Majda, A. J. & Roytburd, V. 1991 Theoretical and numerical structure for unstable one-dimensional detonations. *SIAM Jl Appl. Math.* **51**, 303–343.

Erpenbeck, J. J. 1962 Stability of steady-state equilibrium detonations. *Phys. Fluids* **5**, 604–614.

Erpenbeck, J. J. 1964 Stability of idealized one-reaction detonations. *Phys. Fluids* **7**, 684–696.

Falle, S. A. E. G. 1991 Self-similar jets. *Mon. Not. R. Astr. Soc.* **250**, 581–596.

Falle, S. A. E. G. & Giddings, J. R. 1993 Body capturing. In *Numerical methods for fluid dynamics* (ed. K. W. Morton & M. J. Baines), vol. 4, pp. 337–343. Oxford: Clarendon.

Fickett, W. & Davis, W. C. 1979 *Detonation.* Berkeley, CA: University of California Press.

Fickett, W. & Wood, W. W. 1966 Flow calculations for pulsating one-dimensional detonations. *Phys. Fluids* **9**, 903–916.

Godunov, S. K. 1959 A finite difference method for the numerical computation of discontinuous solutions of the equations of fluid dynamics. *Mat. Sb.* **47**, 357–393.

He, L. & Lee, J. H. S. 1995 The dynamical limit of one-dimensional detonations. *Phys. Fluids* **7**, 1151–1158.

Quirk, J. J. 1994 Godunov-type schemes applied to detonation flows. In *Combustion in high speed flows* (ed. J. Buckmaster, T. L. Jackson & A. Kumar), pp. 575–596. The Netherlands: Kluwer.

Sharpe, G. J. 1997 Linear stability of idealized detonations. *Proc. R. Soc. Lond.* A **453**, 2603–2625.